Wideband Modeling of Power Transformers Using Commercial sFRA Equipment

A. Holdyk, B. Gustavsen, *Fellow, IEEE*, I. Arana, and J. Holboell, *Senior Member, IEEE*

***Abstract*—This paper presents a new procedure to characterize an admittance matrix over a wide frequency band, for the purpose of black-box modeling of power transformers. Unlike previous approaches, our setup is based on a commercial sweep frequency-response analysis measurement instrument which is lightweight and considerably less expensive than dedicated high-precision laboratory equipment. The use of 50-Ω termination resistors allows measuring the terminal admittance matrix without the need for correcting for the measurement cables. The measured admittance matrix is next subjected to rational modeling using vector fitting and passivity enforcement. When applied to a 300-kVA distribution transformer, the resulting model accurately reproduces measured time-domain waveforms.**

***Index Terms*—EMT program, frequency-domain measurements, high-frequency transformer models, model creation and validation, sweep frequency-response analysis (sFRA), time-domain measurements, vector fitting.**

I. Introduction

TRANSFORMER models for detailed medium- and high-frequency studies are not provided as standard information by the transformer manufacturers. If one is interested in the studies of high-frequency transients, voltage transfer, or high-frequency interaction between the transformer and network, then a linear terminal equivalent of the transformer, also called the black-box model, can be used [1]. These models are often based on an admittance matrix formulation, where each element of the matrix is measured either by impulse test or by sweep frequency-response analysis (sFRA). The required measurements are traditionally performed by high-precision instruments, for example, vector network analyzers (VNAs), which are expensive and not very user friendly, and often require additional custom-made equipment [2].

This paper presents a procedure to create and validate a wideband, linear, black-box transformer model using only a commercial, off-the-shelf sFRA measurement system, without any additional equipment. The sFRA devices are designed and used for industrial offline transformer diagnostics and we show how they can also be used for wideband modeling of power transformers. The main advantages of using sFRA equipment in this application are their low cost and ease of use, since these devices are specifically designed to be used with power transformers.

sFRA measurement devices are designed to perform voltage transfer studies on transformers and, thus, have no possibility of measuring current directly, but instead use a shunt resistor. As a result, the measured admittance matrix is not symmetrical and needs to be corrected [3]. This paper shows how to perform measurements of a short-circuit admittance matrix with an sFRA device, how to correct the measured admittance matrix, and how to validate the measurements.

A description of the used measurement system is given in Section II. Section III shows how to perform measurements of an admittance matrix with the sFRA device, and Section IV shows measurements performed on a 300-kVA transformer. Based on these measurements, a pole residue model is developed by a vector fitting routine in Section V. A time-domain validation of that model by means of step voltage measurements is shown in Section VI, followed by a discussion and conclusions.

TABLE I
Technical Specification of the sFRA Instrument

FRA Method	Sweep frequency (SFRA)
(Extended) Frequency range	0.1 Hz – 25 MHz
AO: Measurement voltage at 50 Ω	0.1 – 10 Vpeak-to-peak
AO: Output impedance, Z_{out}	50 Ω
AI: Sampling	100 MS/s
AI: Input impedance Z_{in}	50 Ω
Instrument weight	1.9 kg with battery
Instrument dimensions	250 x 169 x 52 mm

II. sFRA Measurement System

The device used in the study is a sweep frequency-response analysis device designed to detect displacement of windings or faults in the magnetic core of power transformers [4], [5]. This is done by measuring the voltage transfer between transformer terminals over a wide frequency band. It is a relatively small and light device designed specifically for measuring transformers. It has a built-in battery and a Bluetooth adapter so it can be placed close to or at the transformer and connected to it remotely. The device has one analog output (AO) terminal generating a sinusoidal voltage of variable frequency and two analog input (AI) terminals measuring amplitude and phase of the voltage signals. A partial technical specification is shown in Table I.

Manuscript received April 03, 2013; revised August 07, 2013 and October 31, 2013; accepted January 20, 2014. Date of publication February 14, 2014; date of current version May 20, 2014. The work was supported by the Danish PSO as a project 010087 "EMC Wind." Paper no. TPWRD-00380-2013.

A. Holdyk and J. Holboell are with the Technical University of Denmark, Kgs.Lyngby 2800, Denmark (e-mail: aho@elektro.dtu.dk; jh@elektro.dtu.dk).

B. Gustavsen is with SINTEF Energy Research, Trondheim N-7465, Norway (e-mail: bjorn.gustavsen@sintef.no).

I. Arana is with DONG Energy, Gentofte DK-2820, Denmark (e-mail: ivaar@dongenergy.dk).

Digital Object Identifier 10.1109/TPWRD.2014.2303174

Fig. 1. Sweep frequency-response analyzer with dedicated clamps and cables.

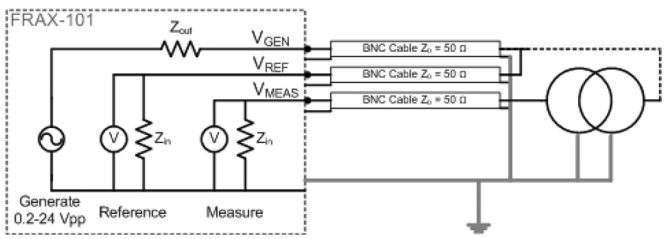

Fig. 2. Internal diagram of FRAX-101 and connection to a transformer.

The measurement system is composed of the sFRA instrument, dedicated cables, and clamps, as shown in Fig. 1. The standard measurement cables are 50-Ω coaxial BNC cables, 18 m long. There are three cables in the set—one for AI and two others are bonded together lengthwise for ease of use; one is used for AI and the other is for AO.

Additional hardware can be purchased, for example, an active impedance probe (AIP) and active voltage probe (AVP), to perform measurements on grounded terminals or when higher input impedance is needed, respectively.

The instrument chassis is shown in Fig. 2 by a dashed line and its internal circuit diagram is shown inside. The instrument generates a sinusoidal voltage at the analog output V_{GEN} and measures the magnitude and phase of a voltage at analog inputs V_{REF} and V_{MEAS}. V_{GEN} and V_{REF} are both connected to the same measuring clamp and, thus, V_{REF} measures the applied voltage directly at the selected terminal of the transformer. V_{MEAS} measures voltage at the other terminal. If one wishes to measure impedance or admittance, the voltage V_{MEAS} can be recalculated to current via the internal impedance of the instrument Z_{in}, which terminates the BNC cable with a matching impedance of 50 Ω:

$$I_{\mathrm{MEAS}} = \frac{V_{\mathrm{MEAS}}}{Z_{\mathrm{in}}} = \frac{V_{\mathrm{MEAS}}}{50}. \tag{1}$$

A single sweep measurement with standard settings takes around 40 s. The details of how to measure the short-circuit admittance matrix of a transformer by the sFRA device are given in the next section.

III. Measurements of Admittance Matrix Elements and Correction Procedures

A black-box model of a transformer can be formulated by the relationship between terminal voltages $V(s)$ and currents $I(s)$ in the frequency domain:

$$I(s) = Y(s) \cdot V(s). \tag{2}$$

For a transformer with n terminals with ground as reference, the admittance matrix will have $n \cdot n$ elements. Then, (2) becomes

$$\begin{bmatrix} I_1(s) \\ \cdots \\ I_i(s) \\ I_j(s) \\ \cdots \\ I_n(s) \end{bmatrix} = \begin{bmatrix} Y_{11}(s) & \cdots & Y_{1i}(s) & Y_{1j}(s) & \cdots & Y_{1n}(s) \\ \cdots & \cdots & \cdots & \cdots & \cdots & \cdots \\ Y_{i1}(s) & \cdots & Y_{ii}(s) & Y_{ij}(s) & \cdots & Y_{\mathrm{in}}(s) \\ Y_{j1}(s) & \cdots & Y_{ji}(s) & Y_{jj}(s) & \cdots & Y_{jn}(s) \\ \cdots & \cdots & \cdots & \cdots & \cdots & \cdots \\ Y_{n1}(s) & \cdots & Y_{ni}(s) & Y_{nj}(s) & \cdots & Y_{nn}(s) \end{bmatrix} \times \begin{bmatrix} V_1(s) \\ \cdots \\ V_i(s) \\ V_j(s) \\ \cdots \\ V_n(s) \end{bmatrix}. \tag{3}$$

Each element of Y can be directly measured in the frequency domain. If $Y_{ij}(s)$ is to be measured, a sinusoidal voltage waveform should be applied to terminal j and the current should be measured at terminal i, keeping all terminals, except terminal j grounded. If all measurements are performed properly, this procedure results in matrix $Y(s)$ being symmetrical. This direct measurement of Y is not possible using the sFRA instrument since the current at terminal i is measured using a 50-Ω shunt resistor, which means that the voltage at this terminal does not equal zero. A correction procedure is therefore necessary to obtain a symmetrical matrix. The procedure's details are presented below.

A. Diagonal Elements of Y(S)

Diagonal elements of $Y(s)$ are normally measured one by one by applying a voltage to a terminal and measuring the current flowing into the same terminal, keeping all other terminals grounded. This cannot be done directly with the sFRA instrument alone. There are, however, two methods to measure diagonal elements with the instrument. One can either purchase and use an active impedance probe (AIP) or use the instrument with a nonstandard connection type. In this paper, we use the latter approach, which is shown in Fig. 3.

The measurement is done by applying V_{GEN} to a chosen terminal, for example, terminal i. V_{REF} is measured at the same terminal and V_{MEAS} is connected to ground. The shields of both clamps V_{MEAS} and V_{REF} are connected together and not grounded. The sFRA instrument is disconnected from the mains

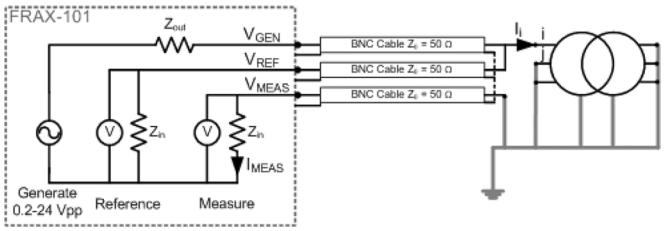

Fig. 3. Connection diagram for an alternative way of measuring diagonal elements of $Y(s)$.

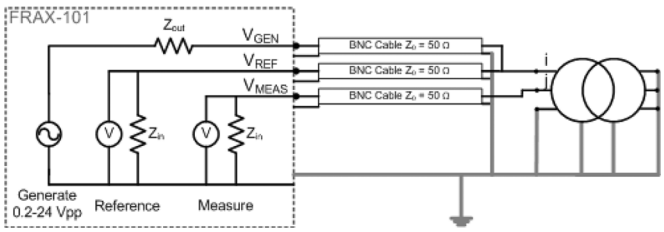

Fig. 4. Connection diagram for measuring offdiagonal elements of $Y(s)$.

and its box is not grounded; the device is floating. That causes the current flowing into the transformer terminal I_i to be the same as the current flowing into the instrument $\mathrm{I_{MEAS}}$, which is equal to $(V_{\mathrm{MEAS}})/(Z_{\mathrm{in}})$. The voltage at the measured terminal is equal to the voltage difference $V_{\mathrm{REF}} - V_{\mathrm{MEAS}}$ and, thus, the measured self-admittance of terminal i is

$$Y_{ii}(s) = \frac{V_{\mathrm{MEAS}}(s)}{Z_{\mathrm{in}} \cdot (V_{\mathrm{REF}}(s) - V_{\mathrm{MEAS}}(s))}. \tag{4}$$

B. Offdiagonal Elements of Y(s)

Offdiagonal elements of $Y(s)$, for example, $Y_{ji}(s)$ are obtained by applying $V_{\mathrm{GEN}}(s)$ to terminal i and measuring $V_{\mathrm{MEAS}}(s)$ at terminal j, as shown in Fig. 4.

In this arrangement, the current flowing into terminal j, $I_j(s)$ is measured with shunt resistorZ_{in}, which causes the voltage at this terminal to be nonzero. The effect of Z_{in} is eliminated by following the approach in [3]. From (3), one can calculate

$$I_j(s) = Y_{ji}(s)V_i(s) + Y_{jj}(s)V_j(s) \tag{5}$$

$$Y_{ji}(s) = \frac{I_j(s)}{V_i(s)} - Y_{jj}(s)\frac{V_j(s)}{V_i(s)}. \tag{6}$$

$Y_{ji}(s)$ from (6) is a result of a measurement shown in Fig. 4, and it contains not only the mutual admittance between terminals j and i, $(I_j(s))/(V_i(s))$ but also the part related to self admittance of terminal j, namely, $Y_{\mathrm{jj}}(s)(V_{\mathrm{j}}(s))/(V_{\mathrm{i}}(s))$. Therefore, the result obtained from the measurement shown in Fig. 4 is not a proper mutual admittance between terminals i and j. If we name the admittance obtained from the measurement in Fig. 4 $\tilde{Y}_{\mathrm{ji}}(s)$ and the pure mutual admittance between terminals j and i $Y_{ji}(s)$, then after (6), the pure mutual admittance between terminals, j and i is

$$Y_{ji}(s) = \tilde{Y}_{ji}(s) + Y_{jj}(s)\frac{V_j(s)}{V_i(s)}. \tag{7}$$

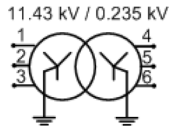

Fig. 5. Terminal connections of the measured transformer.

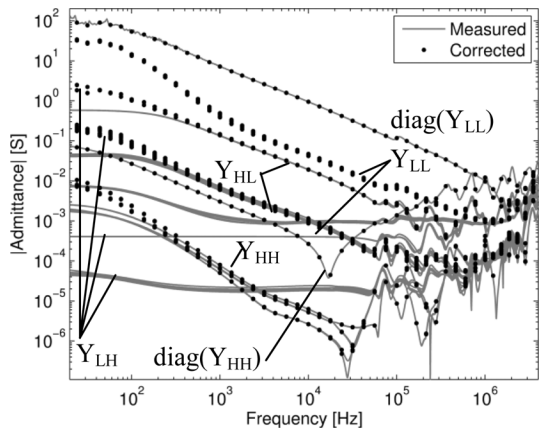

Fig. 6. Magnitude of measured admittances and corrected elements of Y.

Therefore, in order to obtain a proper value of mutual admittance by the sFRA instrument, one has to recalculate (correct) the measured admittances according to

$$Y_{ji}(s) = \frac{V_{\mathrm{MEAS}}(s)}{Z_{\mathrm{in}} \cdot V_{\mathrm{REF}}(s)} + Y_{jj}(s) \cdot \frac{V_{\mathrm{MEAS}}(s)}{V_{\mathrm{REF}}(s)} \tag{8}$$

where $Y_{jj}(s)$ is the previously measured value of the self admittance at terminal j.

IV. Measurements of a Transformer

The measurement procedure described in Section III was performed on a 300-kVA, 11.43/0.235-kV Ynyn0 transformer, shown in Fig. 5.

The original instrument's cables connecting the box with measuring clamps were substituted with three separate 4-m-long BNC cables. The influence of cables on the measurements is described in Section VII. The measurements were made at logarithmically spaced frequencies between 20 Hz and 4 MHz.

The measured admittance matrix can be represented by four submatrices representing the voltage levels of a transformer, H—high voltage and L—low voltage, as shown

$$\begin{bmatrix} I_H \\ I_L \end{bmatrix} = \begin{bmatrix} Y_{HH} & Y_{HL} \\ Y_{LH} & Y_{LL} \end{bmatrix} \cdot \begin{bmatrix} V_H \\ V_L \end{bmatrix} \tag{9}$$

where each of the admittance submatrices is of dimension 3×3.

Fig. 6 shows the frequency-dependent magnitude of all elements of the measured admittance matrix together with corrected offdiagonal elements.

The change to the magnitude of the offdiagonal elements of Y_{LL} and Y_{LH} by the correction is significant for all frequencies. The magnitude of elements of Y_{HH} and Y_{HL} is changed only at lower frequencies where the associated impedance is smaller than, or comparable to 50 Ω.

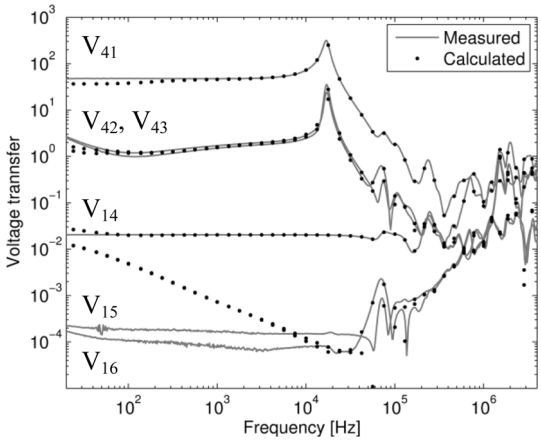

Fig. 7. Measured and calculated voltage transfers.

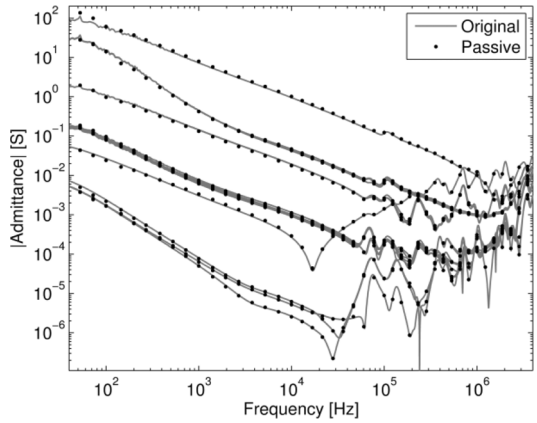

Fig. 8. Elements of admittance matrix Y—original and after approximation with vector fitting.

The performed measurements and corrections can be validated by calculating the voltage ratio between terminals and comparing them with direct measurements. The voltage ratio between the HV side and LV side can be calculated by

$$V_{HL} = -Y_{HH}^{-1} Y_{HL}. \tag{10}$$

And the voltage ratio between the LV side and HV side is

$$V_{LH} = -Y_{LL}^{-1} Y_{LH}. \tag{11}$$

Fig. 7 shows the measured and calculated voltage transfer from the HV side to the LV side (between terminals 1 and 4—V_{14}, 1 and 5—V_{15}, 1 and 6—V_{16}) and from the LV side to the HV side (between terminals 4 and 1—V_{41}, 4 and 2—V_{42}, 4 and 3,—V_{43}).

The measurement of the voltage ratio was performed directly at the transformer terminals using a vector network analyzer (VNA) instrument and voltage probes. Here, an Agilent E5061B VNA was used. The measured voltage ratio at 50 Hz is $V_{LH} = V_{41} = 47.37$ and $V_{HL} = V_{14} = 0.02045$, and the values calculated from a model are: 36.72 and 0.02211, respectively. The error is maximum at low frequencies; at 50 Hz, it is, 29% for V_{LH} and 7.5% for V_{HL}. High accuracy is obtained above approximately 20 kHz for V_{LH} and above 200 Hz for V_{HL}. The biggest deviation is found for V_{LH}, which is associated with open LV terminals of the transformer (11). This inaccuracy is due to the large impedance mismatch between the transformer terminal and the sFRA instrument's AO/AI terminals. This will be explained in Section VII.

V. Creation of a Model

Three steps need to be performed in order to create a representation of (3) which can be used in time-domain simulations in electromagnetic transients programs: 1) a mathematical approximation of (3) needs to be found; 2) passivity of the approximation has to be ensured guaranteeing stable time-domain simulation, and 3) the passive approximation of (3) needs to be described in a way which allows incorporation into electromagnetic transients program. To perform all three steps we used the freely available matrix fitting toolbox (MFT) [6] which is based on vector fitting (VF) [7] as well as passivity enforcement by residue perturbation [8].

The output of the VF routine is a symmetrical rational model on pole-residue form (12), with stable poles

$$Y(s) \cong Y_{\mathrm{rat}}(s) = \sum_{m=1}^{N} \frac{R_m}{s - a_m} + D + sE. \tag{12}$$

MFT assumes that the admittance matrix is symmetrical, which is often not the case, as small discrepancies in measurements can occur. Therefore, the symmetry was enforced, and the admittance matrix was subjected to an approximation using $N = 65$ poles with good results.

The next step is to check whether the obtained model is passive and, if not, to enforce passivity. For the symmetrical model, this implies that

$$\mathrm{eig}(\mathrm{Re}\{\mathbf{Y_{rat}}(s)\}) > 0 \tag{13}$$

$$\mathrm{eig}(\mathbf{D}) > 0. \tag{14}$$

Fig. 8 shows a comparison of the original model and after passivity enforcement and Fig. 9 shows the eigenvalues of the real part of Y before and after passivity enforcement. In order to decrease the passivity violation, the model was limited to frequencies above 40 Hz. It can be seen that the passivity enforcement had an influence on elements of Y in the low-frequency range; however, the approximation is still good.

In Fig. 9, one can notice that the passivity violation was small, mostly in low frequencies, and Fig. 10 shows voltage transfers as calculated from the model with passivity enforcement.

Finally, the passive six-terminal model was represented by a combination of lumped resistance, inductance, and capacitance elements described in a text file, which allows including it directly in the electromagnetic transients program, Alternative Transients Program (ATP-EMTP).

VI. Time-Domain Validation

Four time-domain measurements and simulations were performed and compared in order to validate the model. In each case, a low-amplitude voltage step was applied to one terminal

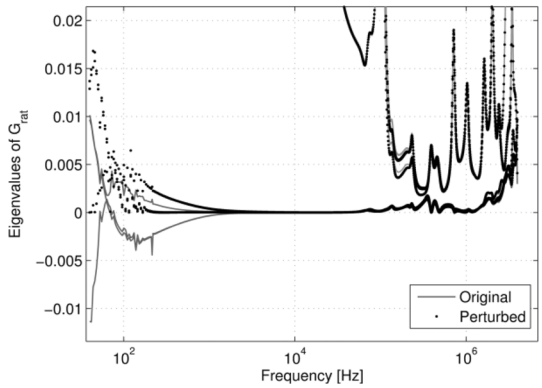

Fig. 9. Eigenvalues of conductance of Y before and after passivity enforcement.

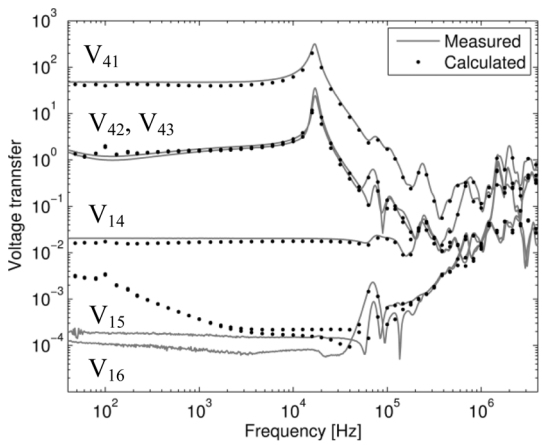

Fig. 10. Voltage transfer after passivity enforcement.

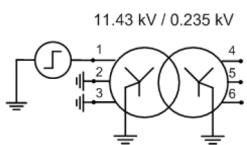

Fig. 11. Voltage step applied to the HV side.

of the transformer with a function generator and measured together with the voltages on the other side by an oscilloscope Tektronix DPO4054P and passive voltage probes TPP1000.

The voltage step function used for excitation of the model in the ATP-EMTP simulations is realized with a controlled voltage source and the measured voltage signal. In this way, the same testing voltage waveform in simulations as in measurements is ensured. In addition, the other terminals in the simulations were subjected to the same terminal conditions as in the measurements.

Several different terminations were chosen to fully test the model's capabilities. Fig. 11 shows a voltage step applied to terminal 1 at the high-voltage side, and the time-domain response to the voltage step is shown in Fig. 12.

The submatrices Y_{HH} and Y_{HL} are tested in this arrangement. All frequencies of the oscillations are properly represented. The dominating frequency of oscillation is around 2 MHz and the model has been developed up to 4 MHz. The amplitude of V_4 for frequencies above around 500 kHz is

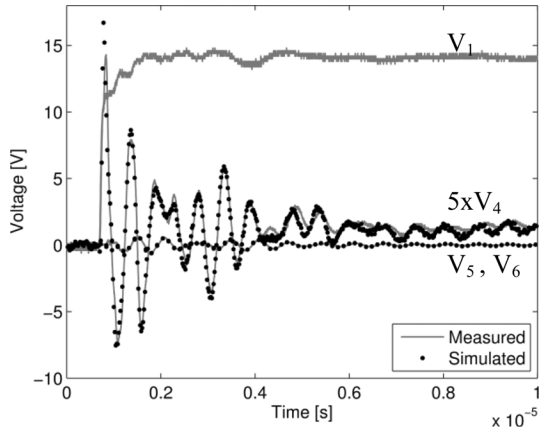

Fig. 12. Time-domain response to the voltage step on the HV side with the LV side opened. V_1 depicts both simulated and measured signal.

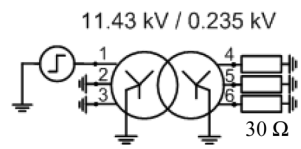

Fig. 13. Voltage step applied to the HV side. The LV side is grounded by 30-Ω resistors.

slightly higher than measured, representing too small attenuation in this frequency bandwidth.

Next, we apply the voltage step to the same terminal but ground the LV terminals through 30-Ω resistors, as shown in Fig. 13. This emulates a situation where a cable of 30-Ω characteristic impedance is connected to the LV side of the transformer. The applied/used 30 Ω is within the range of the characteristic impedance of a typical LV distribution cable.

It is observed that even when the transformer is loaded, the frequencies are properly represented in the simulation, as shown in Fig. 14. Similarly as in the previous case, the damping is too low in the frequencies above approximately 500 kHz. In addition, for frequencies below approximately 300 kHz, the magnitude of simulated V_4 is up to 13 % smaller than the measured value.

Next, in order to test all of the submatrices of Y simultaneously, we load all terminals, as shown in Fig. 15.

As shown in Fig. 16, the frequencies of oscillations are still properly represented although the attenuation at frequencies above approximately 250 kHz is slightly higher than for the measured signals.

The next simulation shows a situation where the voltage step is applied to an LV terminal and the HV terminals are opened, as shown in Fig. 17.

In this case, the frequency of oscillations is much lower than in previous cases with the prevailing frequency of 16.8 kHz; see Fig. 18.

This frequency corresponds exactly with the main resonance frequency shown in Fig. 10. The frequency as well as magnitudes of voltages V_2 and V_3 are properly represented in all simulations. However, the magnitude of simulated V_1 is approximately 20% smaller for the entire simulation. This corresponds to results shown in Fig. 7, where the largest inaccuracy was

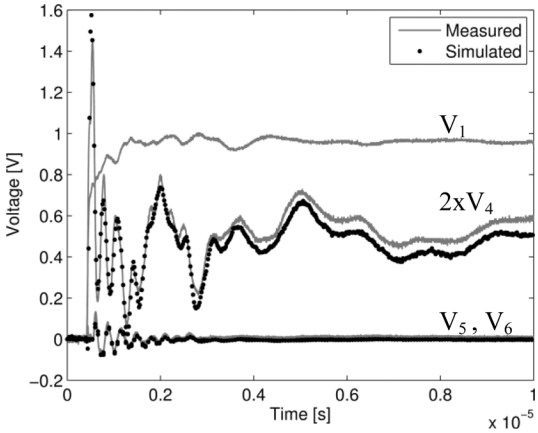

Fig. 14. Time-domain response to the voltage step applied to the HV side. LV side grounded by 30-Ω resistors. V_1 depicts the simulated and measured signal.

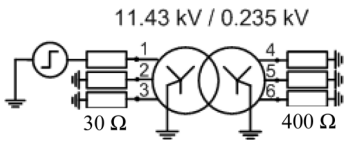

Fig. 15. Voltage step applied on the HV side through the 30-Ω resistor. All other terminals grounded through 400-Ω resistors.

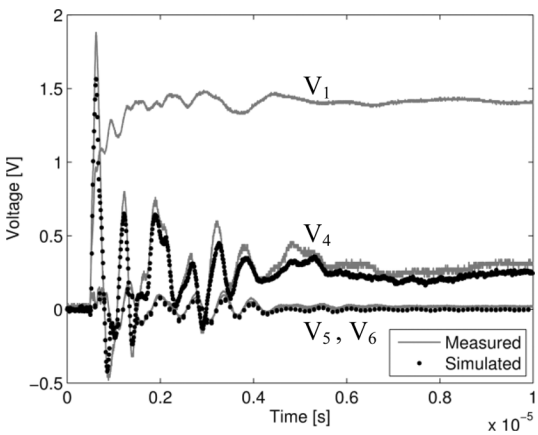

Fig. 16. Time-domain response to a voltage step on the HV side applied through a 30-Ω resistor. All other terminals are grounded through 400-Ω resistors. V_1 depicts the simulated and measured signal.

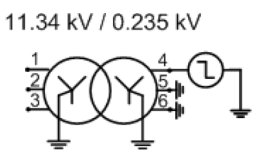

Fig. 17. Voltage step applied to the LV side.

found in V_{LH} and in Fig. 10, where the accuracy was further reduced after the passivity enforcement procedure. The accuracy for the open-circuit state, as is the condition under voltage transfer investigations, can be significantly improved by incorporating direct open-circuit voltage transfer measurements into the admittance matrix Y, as in [2]. That procedure, however, requires performing measurements with additional measurement equipment, which violates the assumption for this study of using only the sFRA instrument.

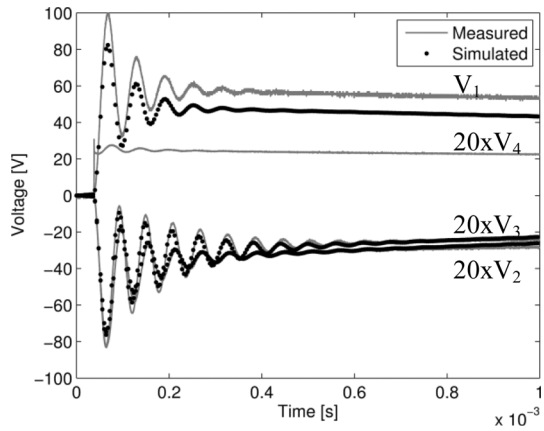

Fig. 18. Time-domain response to a voltage step applied to the LV side with the HV side opened. V_4 depicts the simulated and measured signal.

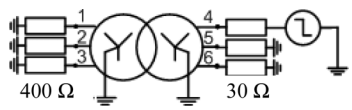

Fig. 19. Voltage step applied on the LV side through the 30-Ω resistor. All other terminals are grounded through 400-Ω resistors.

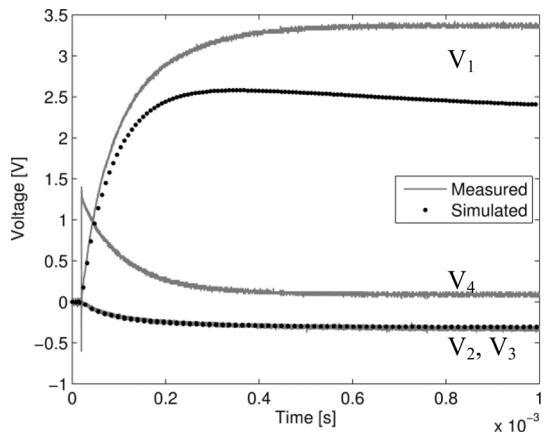

Fig. 20. Time-domain response to a voltage step on the LV side applied through a 30-Ω resistor. All other terminals are grounded through 30-Ω resistors. V_4 depicts the simulated and measured signal.

The final simulation shows a case when a signal is applied to LV terminal through a 30-Ω resistor and all other terminals are grounded through 400-Ω resistors, as shown in Fig. 19.

One can notice in Fig. 20 a significant impact of the resistor loads on the simulated responses. The responses seem to be in agreement with the measurement results for frequencies above the resonance frequency. At lower frequencies, the attenuation is higher than in the measurements.

VII. Discussion

The presented method for linear wideband modeling is general and can be used for multiterminal electrical components or systems. The application of the method to transformers, as shown in this paper, is especially important because it is often the only way to obtain an accurate wideband terminal model for studies in electromagnetic transients programs. Measuring the full short-circuit admittance matrix of a three-phase two-

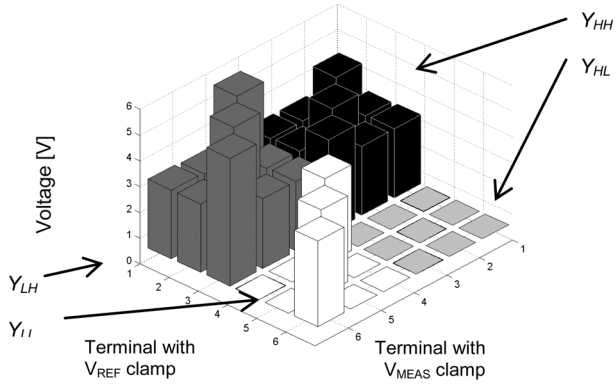

Fig. 21. Magnitude of voltage V_{REF} generated by the sFRA instrument at 50 Hz for all elements of Y.

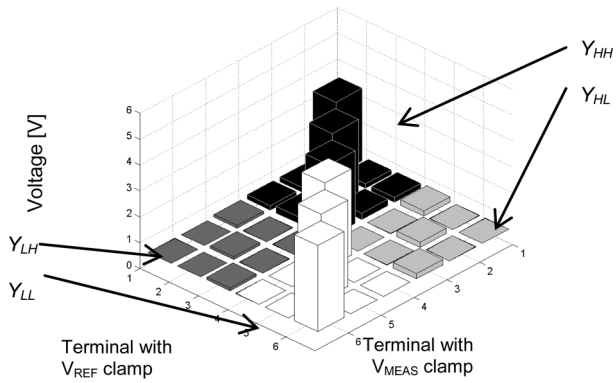

Fig. 22. Magnitude of voltage V_{MEAS} measured by the sFRA instrument at 50 Hz for all elements of Y.

winding transformer requires performing 36 measurements and takes two skilled technicians 2-5 h, depending on the transformer size.

A. Accuracy at Low Frequencies

Section III explained that offdiagonal elements of the admittance matrix need to be corrected, and the correction is dependent on the diagonal elements of Y in the same matrix row.

It is clear that all elements, and especially the diagonal ones, need to be measured very accurately; otherwise, an error from one measurement can propagate to others. Fig. 6 showed the measured and corrected elements of Y. The influence of the transformer's core is minimized for short-circuit measurements; therefore, the impedance of a transformer can be very small in low frequencies, much smaller than the output impedance of the sFRA instrument $Z_{\mathrm{out}} = 50\ \Omega$. In such cases, the voltage generator is too weak to supply a voltage that is high enough to allow accurate measurement. This is shown in Fig. 21, where the voltage generated at the LV terminals, that is, in all elements of submatrices Y_{LL} and Y_{HL}, except diagonal elements, is very low. A further difficulty arises from the fact that the contact resistances may introduce noticeable errors in these measurements. It is therefore essential to have very good contacts between measuring clamps and terminals in order to minimize the inaccuracies.

On the other hand, one can see in Fig. 22 that due to the voltage ratio of the transformer (11.43/0.235 kV), the induced voltage on the LV side is very low when the V_{REF} is applied to the HV side. One can therefore observe a very low value of the measured voltage at 50 Hz for the terminals 4–6. This might result in inaccuracies in the submatrix Y_{LH}.

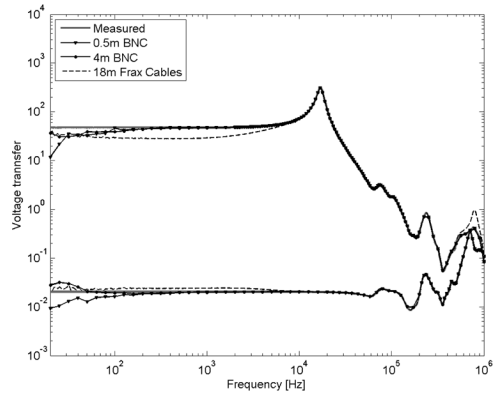

Fig. 23. Comparison of voltage transfers calculated from the models based on measurements made by different coaxial cables.

B. Influence of Cables

It is known that the cables' capacitance may influence the elements of the measured Y by shifting the measured response in frequency. If that was the case, one would have to correct the measured admittances by the cable capacitance. This is; however, not the case with the used sFRA instrument, as shown in Fig. 23.

The figure shows the voltage transfer calculated from models based on measurements made with coaxial cables of three different lengths: 0.5, 4, and 18 m—sFRA instrument's original cables. It is clear that all resonance frequencies are the same and, therefore, it might be stated that the cables' length does not influence the measurements. This is due to two reasons. The sFRA instrument's input/output impedance Z_{in} and Z_{out} match the characteristic impedance of all measurement cables. Another reason comes from (4) and (8), which describe calculations of elements of the admittance matrix from V_{REF} and V_{MEAS}. For clarity, they are repeated below

$$Y_{ii}(s) = \frac{V_{\mathrm{MEAS}}(s)}{Z_{\mathrm{in}} \cdot (V_{\mathrm{REF}}(s) - V_{\mathrm{MEAS}}(s))} \tag{15}$$

$$Y_{ji}(s) = \frac{V_{\mathrm{MEAS}}(s)}{Z_{\mathrm{in}} \cdot V_{\mathrm{REF}}(s)} + Y_{jj}(s) \cdot \frac{V_{\mathrm{MEAS}}(s)}{V_{\mathrm{REF}}(s)}. \tag{16}$$

In our case, if we assume that cables have the same influence on V_{REF} and V_{MEAS} (cables are identical), then this influence will cancel each other out during the admittance calculation since it will be the same in the numerator and denominator. However, if the cables are not identical, thus the influence on V_{REF} and V_{MEAS} is different, then an error will occur. This is seen in Fig. 23 where the voltage transfer measured with the FRAX-101's original cables differs from the others for frequencies up to 100 kHz.

For the sFRA instrument's original cables, the cable with generated voltage V_{GEN} and the cable with reference voltage V_{REF} were glued together lengthwise for simplicity of use, as shown in Fig. 24 and also visible in Fig. 1, to the right. Due to this arrangement, there is a mutual inductance between two cables,

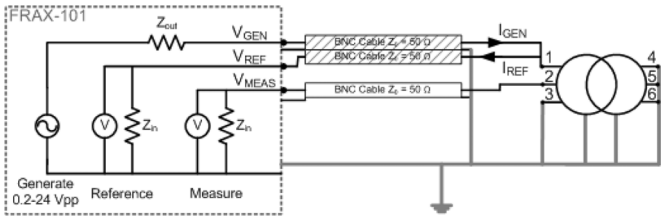

Fig. 24. FRAX-101 connection diagram showing cables V_GEN and V_REF glued together lengthwise.

which is visible up to 100 kHz, when the screens start shielding perfectly. This mutual inductance is frequency dependent and changes V_{REF} but does not influence V_{MEAS}, which results in incorrect values of elements of Y for frequencies at which the two glued cables influence each other. It is therefore recommended to use separate cables for measurements of the admittance matrix.

VIII. Conclusion

This paper presents a complete procedure to create and validate a wide frequency band model of a power transformer using commercial sFRA measurement equipment. In principle, the method can be used for any sFRA instrument of comparable construction as used in the study, that is, measuring the current via shunt resistors.

The main advantages of using sFRA equipment is its price, being many times lower than for high accuracy equipment (e.g., vector network analyzers) and its ease of use, since those devices are specifically designed to be used with power transformers. The use of 50-Ω terminations further makes the measured admittances independent on the length of the measurement cables, but causes a need for correction in order to obtain the correct admittance matrix.

It was shown that the created model was accurate for medium and high frequencies, namely, above several kilohertz and up to 4 MHz. At lower frequencies, the model might be less accurate due to very low impedance of the measured transformer compared to the 50-Ω terminations. The resulting model was shown to accurately reproduce transient waveforms at the transformer terminals with alternative terminal conditions. It was further shown that the use of the sFRA instrument's original cables with longitudinally attached output and reference cable influenced the results in frequencies up to 100 kHz due to mutual coupling effects. This problem was overcome by replacing the original cables with independent cables.

References

[1] J. Martinez-Velasco, *Power System Transients. Parameter Determination*. Boca Raton, FL, USA: CRC, 2010.
[2] B. Gustavsen, "Wide band modeling of power transformers," *IEEE Trans. Power Del.*, vol. 19, no. 1, pp. 414–422, Jan. 2004.
[3] B. Gustavsen, "Removing insertion impedance effects from transformer admittance measurements," *IEEE Trans. Power Del.*, vol. 27, no. 2, pp. 1027–1029, Apr. 2012.
[4] CIGRE A2 WG26 (2008), "Mechanical condition assessment of transformer windings using Frequency Response Analysis (FRA). CIGRE, Brochure 342," *ELECTRA*, vol. 237, pp. 34–45, Apr. 2008.
[5] FRAX-101: Sweep Frequency Response Analyzer, 2013. [Online]. Available: www.megger.com
[6] B. Gustavsen, Matrix fitting toolbox, User's Guide and Reference Tech. Rep. 1.0, 2009. [Online]. Available: http://www.sintef.no/vectfit
[7] B. Gustavsen and A. Semlyen, "Rational approximation of frequency domain responses by vector fitting," *IEEE Trans. Power Del.*, vol. 14, no. 3, pp. 1052–1061, Jul. 1999.
[8] B. Gustavsen, "Fast passivity enforcement for pole-residue models by perturbation of residue matrix eigenvalues," *IEEE Trans. Power Del.*, vol. 23, no. 4, pp. 2278–2285, Oct. 2008.

A. Holdyk was born in Poland in 1983. He received the M.Sc. degree majoring in information processing for control from Silesian Technical University, Gliwice, Poland, in 2008, and the M.Sc. degree in wind power–electrical engineering from the Technical University of Denmark (DTU), Kgs.Lyngby, Denamrk, in 2009, where he is currently pursuing the Ph.D. degree in electrical engineering.

His work interests include high-frequency interaction between electrical components and the modeling and simulation of electromagnetic transient phenomena related to offshore wind farms.

B. Gustavsen (M'94–SM'03–F'14) was born in Norway in 1965. He received the M.Sc. and Dr.Ing. degrees from the Norwegian Institute of Technology (NTH), Trondheim, Norway, in 1989 and 1993, respectively.

Since 1994, he has been with SINTEF Energy Research where he is currently a Senior Research Scientist. His interests include the simulation of electromagnetic transients and modeling of frequency-dependent effects. He spent 1996 as a Visiting Researcher at the University of Toronto, Toronto, ON, Canada, and 1998 at the Manitoba HVDC Research Centre, Winnipeg, MB, Canada.

Dr. Gustavsen was a Marie Curie Fellow at the University of Stuttgart, Stuttgart, Germany, from 2001 to 2002.

I. Arana received the B.Sc. degree from ITESM, Mexico, in 2005 and the M.Sc. and Ph.D. degrees in electrical engineering from the Technical University of Denmark, Kgs.Lyngby, Denmark, in 2008 and 2012, respectively.

Currently, he is a Grid Connection Manager at DONG Energy, Gentofte, Denmark. His work interests include protection coordination, electromagnetic transients simulations, and harmonic studies in large offshore wind farms. He has industrial experience in wind turbine manufacturers, energy audit consulting services, and power utilities.

J. Holboell (SM'11) is Associate Professor at the Technical University of Denmark (DTU) with many years of experience involving electric power components, their properties, and high-frequent equivalents plus methods for condition assessment of these components. His past years' focus was on high-voltage transformers and cables and, in general, components performance under ac and dc transients. The work is now concentrated on wind turbine components, materials, and high-voltage research with respect to the future power grid. He has been a Visiting Researcher at Ontario Hydro Research, Canada; Royal Institute of Technology, Sweden; and Monash University, Monash, Australia.

Prof. Holboell is Senior Member of CIGRÉ Study Committee D1.